ried out at NBS (*3*). The recalculation differs from the previously extant equations (*4*) at a level far too small to explain the anomalous results. In addition, a recent experiment which measured in vacuum the mass difference between objects of differing D (*5*) has made it possible to determine ρ directly through Archimedes' principle. No anomalous behavior was observed.

In an effort to reconcile the various results, the Center for Absolute Quantities (CAPQ) undertook a reexamination of the matter. (The CAPQ is responsible for the maintenance of the kilogram mass unit and of the high-accuracy mass measurement capabilities at NBS.) The original data that were used to develop the *Science* report (*1*) were reviewed, and a new experiment was undertaken.

In an analysis of his results after the publication of (*1*), Pontius became aware of a number of defects in the original work not initially obvious, the main one being a break in the chain of certification of the pressure-measuring devices at the high-elevation stations and another being a questionable pressure sensor in the altitude and decompression chambers. Forewarned of these difficulties, we endeavored to avoid whatever systematic errors might have been present in the original study by measuring the experimental parameters as accurately as possible and by maintaining calibrations rigorously traceable to NBS.

Since the effect seemed to occur entirely between normal atmospheric pressure and 80,000 Pa, the findings should be confirmed if the experiments are repeated in a well-equipped laboratory at an elevation of about 1600 m. Such a laboratory exists at Sandia Corporation, Albuquerque, New Mexico. With the cooperation of Sandia staff, CAPQ personnel repeated the experiment with all of the objects listed above and several other stainless steel kilograms with four times the surface-to-volume ratio of the standards. State-of-the-art measurement systems were used wherever possible (*6*).

The comparisons conducted at NBS and Sandia show mass discrepancies between weights with large volume differences which, if attributable to errors in the applied buoyancy corrections, would place an uncertainty on the ρ algorithm of less than 0.04 percent of ρ. This figure, if dependent on barometric pressure, would imply an error in the calculation of ρ of less than 0.2 percent per atmosphere of pressure change and thus within the maximum uncertainty originally expected by Pontius (*1*).

We have not been able to establish in detail the exact point at which the large, unexpected systematic error crept into the initial experiments. The difficulties with pressure measurement mentioned above, the less than ideal thermal conditions at the high-elevation laboratories, and the apparent effect of vibration in the deep-sea decompression chamber all seem possible sources for the introduction of systematic error.

Even though the initial alarm concerning difficulties in comparing masses of different D now seems overstated, significant problems still exist. There remains, for instance, an uncertainty in the mass unit in materials other than platinum (for example, stainless steel) which exceeds the precision of the best kilogram comparators and which is a direct result of presently accepted uncertainties in state-of-the-art buoyancy corrections. At 293.15 K, 101,325 Pa (1 atmosphere), and 50 percent relative humidity, estimated uncertainties in ρ based on our most recent measurements correspond to uncertainties in mass in the transfer between platinum-iridium and stainless steel artifacts (volume difference, ~ 80 cm^3) of approximately 40 μg. This uncertainty may be compared to the precision of the best kilogram comparators, about 1 μg. It is also true that, in order to achieve even this accuracy, a substantial effort is necessary both to measure accurately the properties of air in the balance enclosure and to create stable conditions within the balance case during weighings.

R. M. SCHOONOVER
R. S. DAVIS, V. E. BOWER
Center for Absolute Physical Quantities, National Bureau of Standards, Washington, D.C. 20234

References and Notes

1. P. E. Pontius, *Science* **190**, 379 (1975).
2. The several algorithms extant at the time of the work [for example, (*4*)] agree, for any given set of observables, to within about 0.03 percent of ρ. The cause of the minor variations ranges from minor errors in formulation (in one case) to the choice of values of the constants (the gas constant, R, for example).
3. F. E. Jones, *J. Res. Natl. Bur. Stand.* **83**, 419 (1978).
4. P. E. Pontius, *Mass and Mass Values* (NBS Monograph 133, Government Printing Office, Washington, D.C., 1974); *Smithsonian Meteorological Tables*, R. J. List, Ed. (Publication 4014, Smithsonian Institution, Washington, D.C., ed. 6, 1958).
5. W. F. Koch, R. S. Davis, V. E. Bower, *J. Res. Natl. Bur. Stand.* **83**, 407 (1978).
6. R. M. Schoonover, R. S. Davis, R. G. Driver, V. E. Bower, *ibid.*, **85**, 27 (1980).

26 December 1979

Organic Carbon: Oxidation and Transport in the Amazon River

Abstract. *Spatial and temporal patterns in the organic carbon load (< 1 millimeter) of the Amazon River indicate that oxidation was constant throughout the river at any one time but was much greater at rising water than at high water, whereas transport was constant. The total effective efflux, as the sum of oxidation plus transport in the river, was about 10^{14} grams of carbon per year. Estimates for other river systems suggest that global riverine carbon fluxes exceed 10^{15} grams per year.*

The transport and oxidation of organic carbon in the Amazon River reflect, over long distances, upstream flooding events and the geologic and vegetative structure of the drainage basin (*1*). The sum of the transport and processing fluxes yields the amount of organic carbon effectively exported from Amazonia. The sum for all large rivers constitutes the riverine role in the global carbon cycle. This role is not yet defined. As far as we know, there are no published data for the transport of organic carbon in any major river that encompass the hydrologic year (*2*). Existing data on organic carbon from the Amazon are either from restricted reaches or were taken at only one stage of the hydrologic cycle.

We report results from two cruises of the R.V. *Alpha Helix* which assess for the first time spatial and temporal patterns in the organic carbon load of the Amazon River. Using these data as a model, we then estimate global riverine carbon fluxes. We test three hypotheses, based on the work of earlier investigators (*3*), concerning the sources, utilization rate, and downstream export of organic matter. They hypothesized that changes in the input and utilization of dissolved and particulate organic matter should be predictable on the basis of river size. For very large rivers (order 9 through 12), the hypotheses are as follows:

(i) Swamp hardwood forests and floodplains decompose fine particulate matter during periods of low water; this material is subsequently returned to the rivers by flooding water and surface runoff.

(ii) The relative rates at which organic matter is utilized tend to be constant from the headwaters to the sea in an unperturbed river system.

(iii) The seasonally pulsed nature of organic inputs is damped by biological processes and retention, such that the total exports of organic matter do not increase downstream.

Transect 1 extended 2000 km, from

0036-8075/80/0321-1348$00.50/0

Manaus, Brazil, to Iquitos, Peru, in February to March 1977 (R.J.N. and J.T.B.) at the beginning of the rainy season when water levels were rising about 1 m per week. Transect 2 extended 3400 km, from Iquitos, Peru, to Belem, Brazil, in May to June 1977 (J.E.R., R.C.W., and R.F.S.) during peak flooding when the river inundates terrestrial habitats for several kilometers on each side of the normal channel in upstream reaches to 20 to 100 km in downstream reaches. Chemical measurements included particulate organic carbon < 1 mm (POC), dissolved organic carbon (DOC), the organic matter content of seston, and the respiratory oxidation activity (*4*).

The amount of organic matter present in the fine suspended load averaged about 10 percent during both transects (Table 1) (*5*). The concentration of POC during the rising-water period was 15 to 20 g m^{-3} upriver and decreased to 8.2 g m^{-3} downriver at Manaus, whereas at high water the POC concentration reached an upriver maximum of 3.7 g m^{-3} and exhibited downstream values of 1 to 2 g m^{-3}. During both rising and high water, the DOC concentration was relatively uniform throughout the river, averaging 4.2 and 6.5 g m^{-3}, respectively. The POC and DOC values appear comparable to those of other investigators at single stations with regard to both wet- and dry-season values (*6*). Respiration during rising water was higher by about two orders of magnitude than at high water, averaging 26 and 0.2 mg m^{-3} $hour^{-1}$ throughout the river, respectively. Relative utilization rates (*7*) showed that during rising water 3 percent of the POC pool turned over per day versus about 0.3 percent at high water and that the utilization rate was constant throughout the river. Since an undetermined fraction of the organic carbon pool is refractory, the oxidation of the labile fraction would be more rapid.

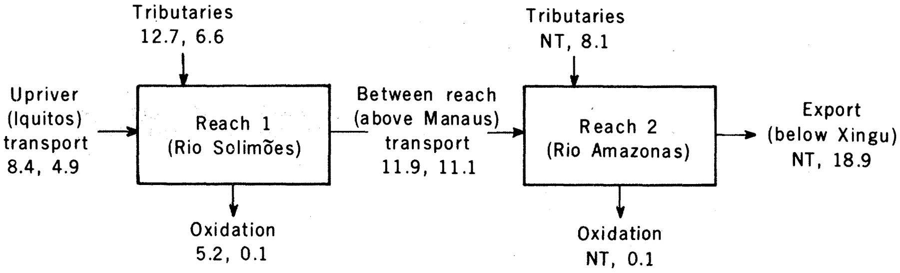

Fig. 1. Evaluation of total organic carbon (< 1 mm POC + DOC) transport and oxidation in two reaches of the Amazon River, from Iquitos, Peru, to just above the confluence of the Solimões with the Rio Negro at Manaus (2200 km), and from Manaus to above the delta region below the confluence with the Rio Xingu (1300 km), at rising water (first number) and peak high water (second number), in grams per second × 10^5 (*NT*, not taken). Inputs to each reach include upriver flows and tributaries (reach 1: Rios Ica, Jutaí, Juruá, Japura, Purus, and Jandiatuba; reach 2: Rios Negro, Madeira, Trombetas, Tapajós, Tocantins, and Xingu). Outputs include downriver transport and oxidation (seston respiration). Data are from Table 1. Transport is given by the concentration multiplied by the discharge; oxidation is given by the respiration rate multiplied by the reach volume, where the volume is the cross-sectional area (discharge/mean velocity) multiplied by the reach length. Inputs and outputs do not balance in all cases because of uncertainty in measurements and possible exclusion of a flux.

What are the sources and fates of the organic carbon in the river which might account for the observed differences in concentration and utilization between rising and high water? The total carbon input to the river reach between Iquitos and Manaus was 21.1 × 10^5 g sec^{-1} at rising water and 11.5 × 10^5 g sec^{-1} at high water, of which 60 percent was from the tributaries and 40 percent was from upriver (Fig. 1). The output from the reach was 17.1 × 10^5 g sec^{-1} at rising water, of which 30 percent was oxidation. Of the high-water output of 11.1 × 10^5 g sec^{-1}, essentially all was down-

Table 1. Organic matter (as the percentage of total seston), POC, DOC, respiration, and river discharge (*5*) for the rising-water cruise, February to March 1977 (transect T1) and the high-water cruise, May to June 1977 (transect T2).

Station	Thalweg* distance above mouth (km)	Organic matter (%)		POC (g m^{-3})		DOC (g m^{-3})		Respiration (mg m^{-3} $hour^{-1}$)		Discharge (m^3 sec^{-1})	
		T1	T2	T1	T2	T1	T2	T1	T2	T1	T2
Napo	3464	8.9	6.3		3.7	4.2	6.7		0.21	35,000	48,000
Pevas	3241	12.7		16.7							
Perua	3167	7.6		19.6		3.9		36.1			
Quebrada Cayarum	3022	7.7		15.6		4.5		31.6			
Leticia	2971		10.0		1.6		5.9		0.23		
Belem	2798										
São Paulo da Olivenca	2732	8.0	10.7	19.6		3.8		29.1		52,000	70,000
Uniao	2664	7.0	12.3	16.2				34.0			
Santo Antônio do Icá	2588	8.0	7.4	20.0	2.0		5.8	10.2	0.18	59,000	80,000
Tonantina	2479	14.0			1.9	4.5			0.24		
Jutaí	2423	8.0	21.5	14.1	1.3	4.0	3.9	24.9	0.22		
Foz do Marmaria	2321			13.5		3.4					
Juruá	2209	7.0		15.8	2.0			29.4	0.24		
Piranhas	2118	12.2		16.8		3.5					
Tefe	1943	7.9		10.2				8.0			
Montivendu	1868										
Coari	1744		21.0	10.4	1.0			20.3	0.24	81,000	110,000
Ilha Jurupara	1670	12.5				3.9					
Purus	1594		8.9		2.5		9.9		0.21		
Anama	1523										
Manacapuru	1403		12.1		1.5	4.8			0.16	96,000	130,000
Solimões	1322	10.0		8.2		6.0		40.8			
Óbidos	870		9.0		2.0				0.22	170,000	230,000
Tapajós	768		10.3		1.6		7.0		0.21		
Xingu	438				1.7				0.17		
Mouth	0										

*Deepest points of a river channel joined by a line.

river transport. Of the 19.2×10^5 g sec^{-1} input to the lower reach at high water, about 60 percent was from upriver and 40 percent was from the tributaries whereas 18.9×10^5 g sec^{-1} was lost to downriver transfer.

Our results reinforce the initial hypotheses of this study. (i) With respect to sources, our data do not directly demonstrate inputs from hardwood forests and floodplains. However, POC concentrations and oxidation were considerably higher at rising than at high water, which suggests that labile organics were being entrained and utilized. These organics could also consist of degradation products of macrophytes (*3*, *8*) and inputs from primary production in bordering varzea lakes (*1*, *9*). Phytoplankton production in the main river is negligible (*10*). Erosion in the Andean highlands supplies some POC (*11*). The DOC in these tropical waters is chemically similar to that of soil humic acids and probably is of terrestrial origin (*12*). (ii) With respect to the utilization rate, the oxidation of organic carbon was relatively constant for a particular flow regime throughout all reaches of the river, but both the respiration rates and the relative utilization rates were much greater during the rising-water period than during high water, presumably a reflection of increased substrate availability. (iii) With respect to downstream export, Gibbs (*11*) has suggested that a downstream decrease in the concentration of total suspended solids during the wet season reflected the dilution of montane waters by less concentrated tropical rivers. Our results showed that the downstream decrease at rising water was due about equally to oxidation and dilution, whereas dilution was the major factor at high water. These observations suggest that retention and consequent oxidation are the major factors reducing sestonic concentrations in the river and providing a uniform downstream export of organics. This research has provided two points on the hydrograph. We hypothesize that the annual sequence of transport and oxidation of carbon is as shown in Fig. 2.

These results have a significant bearing on the interpretation of calculated losses of organic carbon from Amazonia and inputs to the ocean. If the calculated export of carbon (Fig. 1) is used to estimate annual losses, then 6×10^{13} g $year^{-1}$ are exported to the South Atlantic Ocean. However, the data used here are from surface samples, which may not be representative of the sediment suspended through the full depth of the water column. Curtis *et al.* (*13*) found that the velocity-weighted concentration of particles smaller than 53 μm on the high-water cruise was about twice the surface concentration; thus, they cautioned that use of surface samples alone could yield significant errors and suggested that velocity-weighted, depth-integrated values should be used. If the relation hypothesized in Fig. 2 holds, the amount of carbon oxidized within the river is about 50 percent of the amount exported. Furthermore, these data do not include organic carbon > 1 mm in size, which could be a significant fraction of the total (*2*). The effective carbon efflux, as the sum of depth- and velocity-weighted export, oxidation, and carbon fractions > 1 mm, could thus approach three times the efflux measured directly. The effective carbon output from the Amazon could exceed 10^{14} g $year^{-1}$.

Current estimates of the total organic carbon input to the oceans from rivers are about 10^{14} g $year^{-1}$ (*2*). If the transport and oxidation patterns observed in the Amazon hold for other major rivers, the contribution of river ecosystems to global carbon fluxes could be seriously underestimated. We estimate that the total effective organic carbon efflux in the world's rivers might exceed 10^{15} g $year^{-1}$ (*14*). Although controversy persists as to the magnitude of carbon release from the disruption of the terrestrial biosphere (2×10^{15} to 18×10^{15} g $year^{-1}$), it has been assumed that all such losses are to the atmosphere (*15*). Carbon inputs to drainage waters after such land-use practices as clear-cutting, burning, or plowing can, however, be accelerated severalfold (*16*). Our estimate of riverine carbon efflux is large enough to suggest that, since rivers are recipients of terrestrial drainage waters, they could provide a significant pathway for carbon released through human activities.

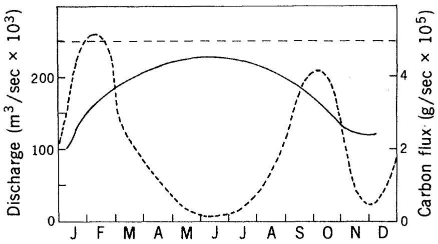

Fig. 2. Hypothesized annual sequence of water discharge (solid line) and carbon transport (dashed line) at the mouth and carbon oxidation (dotted line) throughout the Amazon River. Oxidation of organic carbon increases rapidly with rising flood waters at the beginning of the wet season, as labile organics, partly decomposed during the dry season, are entrained from the riparian habitats. Such ascending flood states are also periods when riverine waters of Andean origin are recharged with inorganic nutrients, which in turn stimulate primary production in floodplain waters. During periods of high discharge, oxidation decreases through the dilution and depletion of labile substances. Oxidation increases again to a secondary maximum as flows subside and organic-rich water from the primary production and biological degradation in the floodplains drains back into the river. At any one time, however, the overall oxidation of organic matter is constant throughout the main river because of a balance between upstream inputs, entrainment, and adequate residence time for downstream utilization. The net result is that export from the river is constant over the hydrologic cycle.

JEFFREY E. RICHEY
Fisheries Research Institute,
University of Washington,
Seattle 98195

JAMES T. BROCK
Department of Biology,
Idaho State University,
Pocatello 83201

ROBERT J. NAIMAN
Woods Hole Oceanographic Institution,
Woods Hole, Massachusetts 02543

ROBERT C. WISSMAR
Fisheries Research Institute,
University of Washington

ROBERT F. STALLARD
Department of Earth and Planetary
Sciences, Massachusetts Institute of
Technology, Cambridge 62139

References and Notes

1. G. W. Schmidt, *Int. Ver. Theor. Angew. Limnol. Verh.* **18**, 613 (1972); E. J. Fittkau, V. Irmler, W. J. Junk, F. Reiss, G. W. Schmidt, in *Tropical Ecological Systems*, F. B. Golley and E. Medina, Eds. (Springer-Verlag, New York, 1975), p. 289; H. Sioli, *Geol. Rundsch.* **66**, 782 (1977); in *Coupling of Land and Water Systems*, A. D. Hasler, Ed. (Springer-Verlag, New York, 1975), p. 199; R. Herrera, C. F. Jordan, H. Klinge, E. Medina, *Interciencia* **3**, 223 (1978).
2. J. R. Sedell and G. E. Likens, in *Measurements of Changes in Carbon Flux and Storage in the Biosphere*, G. E. Likens and D. D. Miller, Eds. (Research Program Development Paper, Energy Research and Development Administration, Washington, D.C., 1978), p. 25.
3. R. L. Vannote, G. W. Minshall, K. W. Cummins, J. R. Sedell, C. E. Cushing, *J. Fish. Res. Board Can.*, in press; R. J. Naiman and J. R. Sedell, *Arch. Hydrobiol.*, in press; R. J. Naiman and J. R. Sedell, *J. Fish. Res. Board Can.* **36**, 17 (1979).
4. We measure oxidation here as seston respiration. On transect 1, we determined the respiration rate by measuring oxygen depletion over 6 hours in a 250-ml bottle dark-incubated at ambient water temperature (29°C). The contents of the bottle were gently stirred and oxygen concentrations were monitored hourly with a Yellow Springs Instrument Company analyzer. The organic matter content was determined gravimetrically after combustion at 525°C, and POC was assumed to be 50 percent of the organic matter. On transect 2, seston respiration rates were estimated from measurements of the activity of the respiratory electron transport system [T. T. Packard, *J. Mar. Res.* **29**, 235 (1971)]. Measurements of POC were made on an elemental analyzer (Perkin-Elmer model 240). Samples were taken 1 m below the surface.
5. R. H. Meade, C. F. Nordin, W. F. Curtis, F. M. Costa Rodrigues, C. M. do Vale, J. M. Edmond, *Nature* (*London*) **278**, 161 (1979).
6. Data, given as suspended solids by R. J. Gibbs [*Science* **156**, 1734 (1967)], can be converted to POC for comparison if one multiplies by 0.05 (10 percent of seston is organic matter, of which 50 percent is carbon), yielding, upriver to downriver, values of 4 to 1 g m^{-3} in wet season. Similarly, G. W. Schmidt [*Amazoniana* **3**, 208 (1972)] found POC concentrations of 3, 2, and 6 g m^{-3} for dry, intermediate, and wet seasons, respectively, near Manaus. P. M. Williams [*Nature*

(London) **218**, 937 (1968)] found dry-season DOC values of 2 to 3.5 $\mathrm{g\ m^{-3}}$ downriver.

7. We assume that biogenic oxidation of organic carbon is mainly associated with POC; thus, relative utilization rates are calculated as POC specific respiration, or grams per cubic meter per day divided by grams per cubic meter (with data from Table 1).
8. C. H. Williams and W. J. Junk, *Biogeographica* **7**, 115 (1976).
9. T. R. Fisher, *J. Comp. Biochem. Physiol.*, in press.
10. R. C. Wissmar, J. E. Richey, R. F. Stallard, J. M. Edmond, in preparation.
11. R. J. Gibbs, *Geochim. Cosmochim. Acta* **36**, 1061 (1972).
12. K. C. Beck, J. H. Reuter, E. M. Perdue, *ibid.* **38**, 341 (1974).
13. W. F. Curtis, R. H. Meade, C. F. Nordin, W. B. Price, E. R. Sholkovitz, *Nature (London)* **280**, 381 (1979).
14. We estimate the POC load in the 20 largest rivers from the data on total suspended solids of H. D. Holland [*The Chemistry of the Atmosphere and Oceans* (Wiley-Interscience, New York, 1978), p. 86] by assuming that the POC is 5 and 2 percent of the total suspended solids in tropical and nontropical rivers, respectively, and that DOC is an average of 4 $\mathrm{g\ m^{-3}}$; these values yield an estimate of 2×10^{14} g $\mathrm{year^{-1}}$ as the input to the oceans. As for the Amazon, corrections for processing and depth-weighting must be applied and organic carbon fractions larger than 1 mm must be included. As the top 20 rivers constitute about 35 percent of the freshwater discharge to the oceans, this estimate would be increased to get the total riverine contribution. The total effective carbon efflux thus is about 10^{15} g $\mathrm{year^{-1}}$.
15. G. M. Woodwell, R. H. Whittaker, W. A. Reiners, G. E. Likens, C. C. Delwiche, D. B. Botkin, *Science* **199**, 141 (1978); W. S. Broecker, T. Taskahashi, H. J. Simpson, T.-H. Peng, *ibid.* **206**, 409 (1979).
16. J. E. Hobbie and G. E. Likens, *Limnol. Oceanogr.* **18**, 734 (1973); D. L. Lush and H. B. N. Hynes, *Hydrobiologia* **60**, 177 (1978); C. Dahm, personal communication.
17. We thank A. H. Devol for assistance with the respiration data, F. Curren and B. Grant for logistics support, and the crew and scientists of the R.V. *Alpha Helix* and the Instituto Nacional Pesquisas Amazonas for their courtesy and cooperation from the National Science Foundation. Supported by grants DEB-76-82631 and BMS-75-07333. Contribution No. 512 from the College of Fisheries, University of Washington, and Contribution No. 9 from the River Continuum project.

20 August 1979; revised 6 December 1979

Alaskan Seismic Gap Only Partially Filled by 28 February 1979 Earthquake

Abstract. *The Saint Elias, Alaska, earthquake (magnitude 7.7) of 28 February 1979 is the first major earthquake since 1900 to occur along the complex Pacific–North American plate boundary between Yakutat Bay and Prince William Sound. This event involved complex rupture on a shallow, low-angle, north-dipping fault beneath the Chugach and Saint Elias Mountains. The plate boundary between Yakutat Bay and Prince William Sound had been identified as a seismic gap, an area devoid of major earthquakes during the last few decades, and was thought to be a likely site for a future major earthquake. Since the Saint Elias earthquake fills only the eastern quarter of the gap, the remainder of the gap to the west is a prime area for the study of precursory and coseismic phenomena associated with large earthquakes.*

On 28 February 1979 an earthquake with surface wave magnitude (M_{S}) 7.7 (*1*) occurred beneath the Chugach and Saint Elias Mountains about 130 km northwest of Yakutat Bay, Alaska. Earlier, the region between the 1958 Fairweather earthquake (M_{S} 7.9), which broke the Fairweather fault as far north as Yakutat Bay, and the 1964 Prince William Sound earthquake (M_{S} 8.4), which ruptured the Aleutian megathrust from about Kodiak Island to Kayak Island, had not been the site of a major earthquake since 1899 and 1900, when four events of M_{S} 8.5, 7.8, 8.4, and 8.1 occurred within 13 months (*2*). Although instrumental control for the epicenters of 1899 and 1900 is almost nonexistent, felt reports and observed uplifts place at least three of them between Yakutat Bay and Kayak Island (*2, 3*). Absence of recent major earthquakes identifies this zone as a seismic gap (*4, 5*), a region of greater potential for major earthquakes than the adjoining regions that have ruptured more recently.

The 28 February 1979 earthquake occurred on the edge of a network of 50 telemetered short-period seismic stations operated by the U.S. Geological Survey in southern Alaska (*6*) as part of its seismic hazard assessment program. The closest station is about 35 km from the epicenter of the main shock, and ten stations are within 100 km at azimuths between 130° and 320° clockwise from north. Readings of P body waves were also obtained from three new Canadian stations in the southern Yukon Territory at distances of 150 to 200 km.

Epicenters determined for the main shock and 102 of the larger aftershocks that occurred within the following 6 days are shown in Fig. 1A. Only solutions with estimated epicentral standard errors less than 10 km, root-mean-square arrival-time residuals less than 1 second, and magnitudes 2.5 or larger are shown. Based on the log number versus magnitude distribution for the aftershocks, the data are probably complete above M_{L} 4.0. Only 42 of the events in Fig. 1A are smaller than M_{L} 3.5.

In contrast to the high rate of aftershock activity, Fig. 1B shows the epicenters of the 37 events that occurred from 1 September 1978 to just before the main shock. The earthquakes shown were selected by the same criteria as the aftershocks. These data are complete, however, above about M_{L} 2.5 and there are only three events above M_{L} 3.5. No foreshock sequence is recognized. The pattern of seismicity is similar to that observed since 1974, when detailed monitoring began, with one exception. The cluster of earthquakes near the southeastern corner of the area outlined by dashes in Fig. 1B occurred during late September in a region without previous high activity. Whether this earthquake swarm is related to the 28 February 1979 event is not known.

The focal mechanism for the main shock, as determined from teleseismic and local P-wave first motions, is shown in Fig. 1A. The steeply dipping plane (strike, N77°E; dip, 79°S) is well constrained, while the gently dipping plane (strike, N105°E; dip, 12°N) is poorly constrained. From regional geology and tectonics and the aftershock distribution (*7*), the gently dipping plane is inferred to be the fault plane and the steeply dipping plane the auxiliary plane. The inferred slip is predominantly reverse dip slip in a north-northwest direction, in close agreement with the direction expected from plate tectonic models (*8, 9*).

Aftershocks that occur within 1 day of a large earthquake are often used to indicate the extent of the rupture zone (*10*). Although 6 days of seismic activity are included in Fig. 1A, the distribution of aftershocks during the first day was not substantially different and gives estimated upper bounds for the rupture dimensions of 65 by 80 km. If the initial rupture area were limited to the northern two-thirds of the indicated aftershock area, which includes the two largest aftershocks and the concentration of events near the U.S.-Canadian border, the rupture dimensions would be approximately 50 by 60 km. In the latter case, the southernmost events would be attributed to secondary faulting triggered by the main shock. Body wave deconvolution suggests that the rupturing was complex, involving at least three rupturing episodes with a combined rupture length of 50 to 70 km.

General constraints on the overall rupture process were determined from fundamental mode Rayleigh waves recorded at the Alaskan stations Palmer (PMR; distance, 425 km; azimuth, 289°) and Shemya (SMY, 2795 km, 272°) and the G_2 surface wave recorded at Uwekahuna, Hawaii (UWE, 4700 km, 199°) (*7*). The results of these analyses, which were performed by standard computational techniques (*11*), are included in Table 1. These results are based on limited data and therefore could not be ade-